Effects of High-Z Limiter/First Wall on the IGNITOR Plasma

R.Zanino

Dipartimento di Energetica, Politecnico, 24 c. Duca degli Abruzzi, 10129 Torino Italy

Report PT DE 501 / IN

January 1999

ABSTRACT

A simple but self-consistent impurity model – SCOUT – has been extended to the toroidal limiter geometry and Mo has been included in the database. The model was validated against experimental data from FTU, showing good agreement with the experiment at medium to high plasma density (≥1e20 m^{-3}). The impurity concentration parameter Z_{eff} and the radiated power fraction in IGNITOR are computed here for different main and edge plasma scenarios, assuming a Mo limiter/first wall.

1. Introduction

Clean plasmas were obtained in high-field high-density limiter experiments, due among others to the screening action of the scrape-off layer (SOL). This could prove to be beneficial also for a high-density limiter tokamak design as IGNITOR [1].

A simple but self-consistent impurity model – SCOUT – was developed [2-4], showing good agreement [5] against experimental data from the Frascati Tokamak Upgrade (FTU) [6] operated with a poloidal Inconel limiter. The model was applied in [7] to a preliminary study of the effects of different limiter materials for IGNITOR, and was validated very recently [8] against experimental data from FTU operated with poloidal or toroidal molybdenum limiter.

Here we shall concentrate on the analysis of IGNITOR operated with Mo FW/limiter.

2. Overview of the SCOUT model

The evolution of a single impurity species in a limiter tokamak plasma is computed, self-consistently coupled to a SOL model (see [8] for a flowchart of the code).

<u>Main plasma</u> (time dependent):
1-D radial model (STRAHL) for impurities. Diffusion and inward pinch, ionization and recombination between different stages. Given plasma background.

<u>SOL plasma</u> (steady state):

- $P_{lim} = P_{in} - P_{rad}^{MAIN} - P_{rad}^{SOL} \rightarrow T_{wall} \rightarrow$ Sputtered influx of neutral impurities Γ_{0Z}.
- Screening efficiency ε of the SOL is computed from LCFS and limiter geometry:
- $(1-\varepsilon)\, \Gamma_{0Z}$ is ionized in the SOL and returns to the limiter
- $\Gamma_Z^{SOL\rightarrow MAIN} = \varepsilon\, \Gamma_{0Z}$ is the source at each time step of the main plasma impurities.
- $\Gamma_Z^{MAIN\rightarrow SOL} + (1-\varepsilon)\, \Gamma_{0Z} \rightarrow$ self-sputtering
- After each time step P_{rad} changes, leading to a new value of P_{lim}, which closes the cycle.

3. Analysis of the IGNITOR case

IGNITOR is a high density limiter tokamak design which should reach ignition (see Table 1).

Table 1 *IGNITOR reference scenario*

Major radius	1.32 [m]
Minor radius	0.47 [m]
Elongation	1.87
Triangularity	0.43
Peak electron temperature	11 [keV]
Average electron temperature	5.5 [keV]
Peak electron density	$11\ 10^{20}$ [m^{-3}]
Average electron density	$5\ 10^{20}$ [m^{-3}]
Edge magnetic safety factor	3.6
Plasma volume (V_p)	10 [m^3]
Plasma surface area (A_p)	34 [m^2]
Alpha power	17.8 [MW]
Ohmic power	9.5 [MW]
Bremsstrahlung power	4.1 [MW]
Cyclotron radiation power	0.5 [MW]

For the main plasma treatment an equivalent minor radius $a_{eq} = 2\ V_p/A_p \sim 0.59$m is assumed here, with circular concentric magnetic surfaces.

The actual FW/limiter and LCMS profiles, from computed equilibrium data [Airoldi and Cenacchi] are used for the SOL plasma treatment as shown in Fig.1. All needed information is taken from a file (see Appendix A) containing a discretization of FW and LCMS poloidal profiles above the mid-plane.

The edge plasma density $n_e(a)$ is fixed and taken either as 1.47e20 or 2.0e20 m^{-3} (see Section 4.2 below).

The evolution of the transient is followed for a fixed maximum number of time steps (typically ~2000-10000) unless a steady state is reached. On Windows 95 or NT the memory needed by a run tends to increase during the execution (apparently because of output on files for evolution diagnostics) by ~O(10kB) at each time step. The reason for this behavior is not clear and on Windows NT it prevented the practical use of more than 4000-5000 steps. On

Unix systems, on the other hand, the memory needed does *not* increase. A 10000 steps run on a Pentium laptop (Windows 95) with 200MHz clock and 64 MB RAM required ~30 hrs, while on a Digital Alpha (Unix) workstation with 433MHz clock and 512 MB RAM it required ~160 mins.

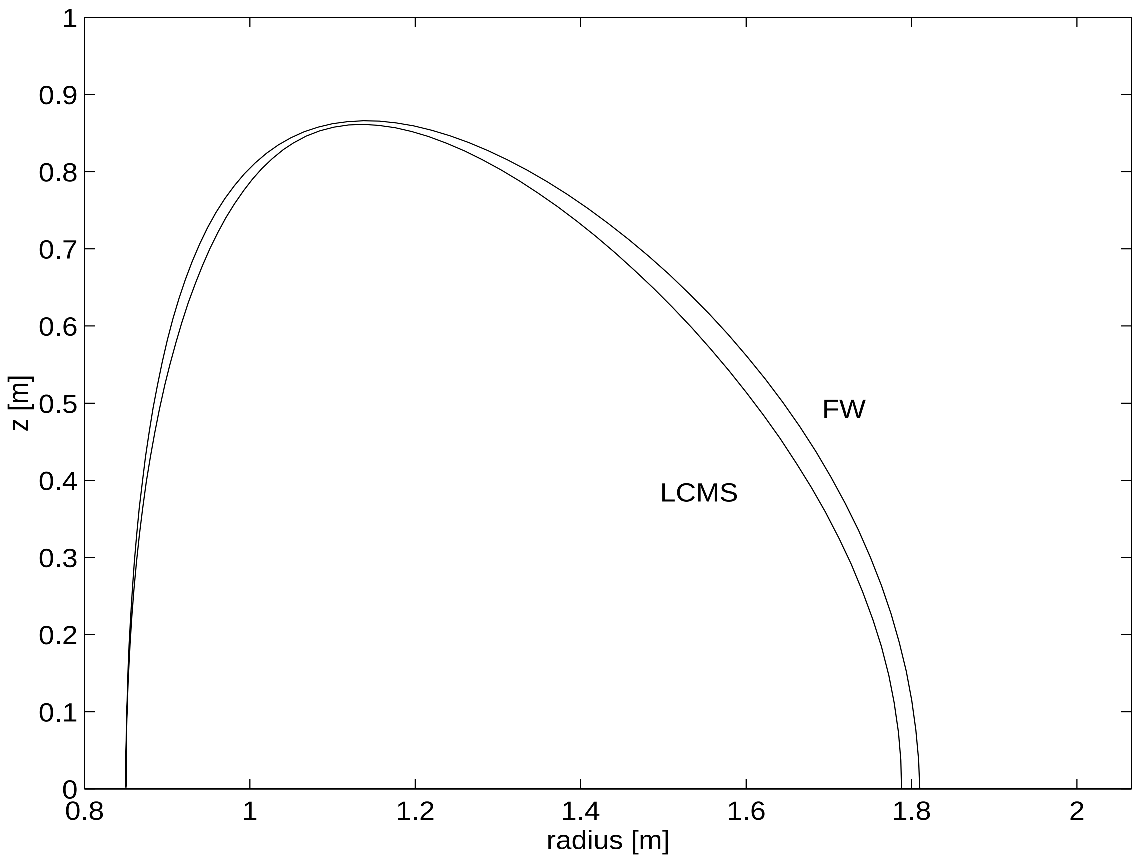

Figure 1 *Reconstruction of poloidal cross section of FW/limiter and LCMS in IGNITOR, as used in the SOL simulations.*

The background electron density and temperature in the main plasma are taken as shown in Figs. 2 and 3 respectively. In particular, the temperature profile was parameterized as in [8] while the density was either parameterized as in [8], using the values of Table 1, or else taken from [9].

Further assumptions need to be made concerning the diffusion coefficient D(r), and the inward pinch velocity V_{in}(r) of the impurities. The radial profiles used in the present study can be found in Fig.4 below.

Finally, in order to simplify the computation, input power and fixed losses are switched on adiabatically over the first 0.1 s.

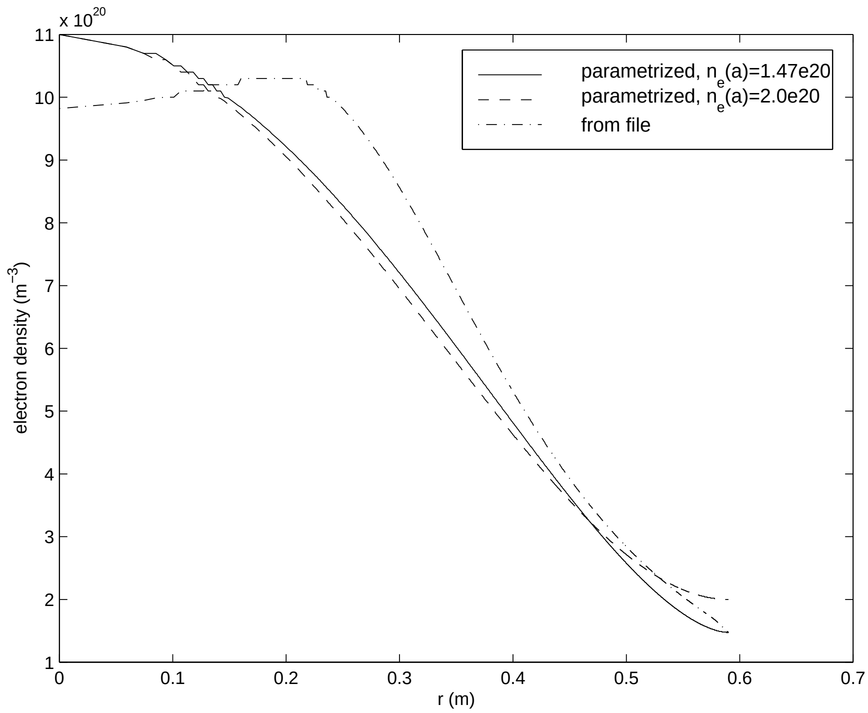

Figure 2 *Electron density profiles assumed in main plasma.*

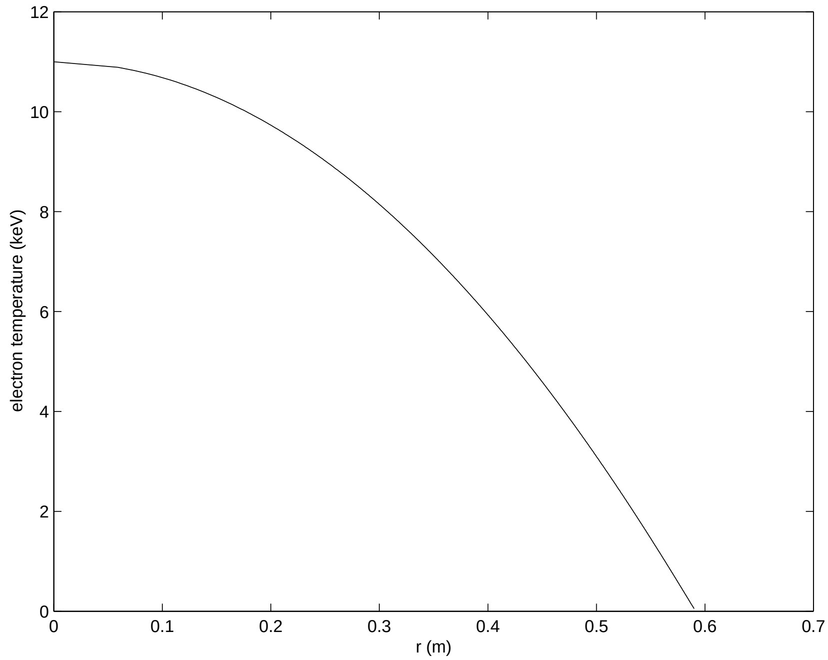

Figure 3 *Electron temperature profile assumed in main plasma.*

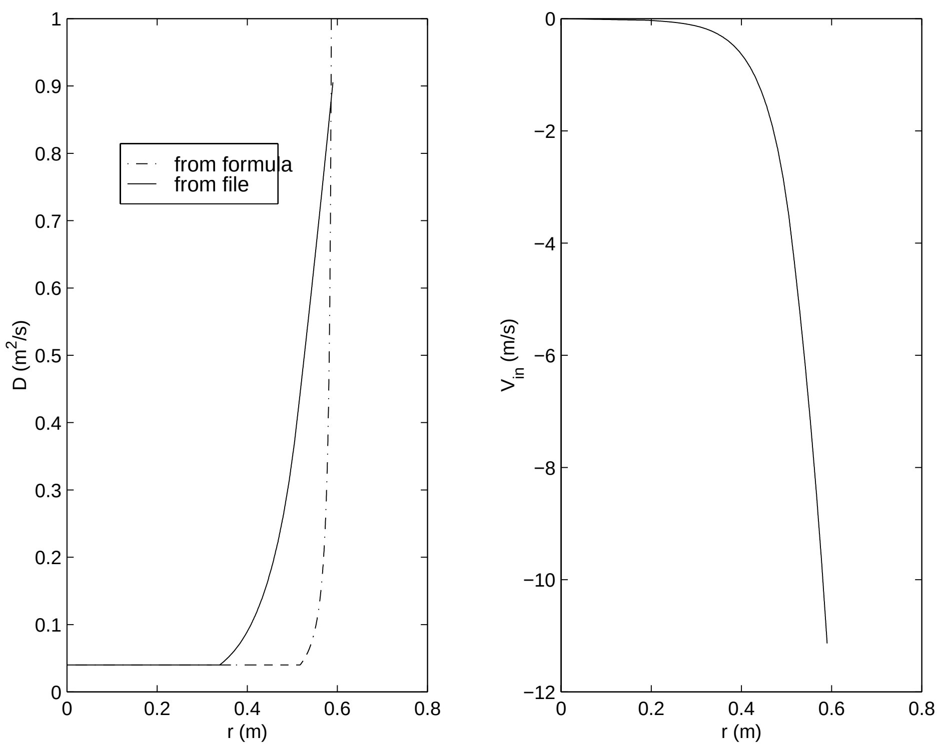

Figure 4 *Radial profiles of impurity diffusion coefficient D(r) and of inward pinch velocity $V_{in}(r)$ assumed in main plasma.*

4. Results

A summary of the results obtained with SCOUT for different scenarios, number of nodes in the radial discretization of the main plasma, and/or number of time steps is given in Table 2.

Table 2 *Summary of results (“**steady state**” in boldface)*

Case	**$n_e(a)$ (m^{-3})**	**Nodes**	**t_{END} (s)**	**T(a) (eV)**	**E_{cons} (%)**	**$\langle Z_{eff} \rangle$**	**P_{rad}^{MAIN} (MW)**	**X_{rad}^{MAIN} (%)**	**P_{rad}^{SOL} (MW)**
$D(r)$, $n_e(r)$ from file (reference)	1.47e20	1001	0.305	49.8	23	1.11	6.2		11.3
=	=	=	0.432	49.0	24	1.13	8.3		9.6
=	**=**	**=**	**0.540**	**48.7**	**20**	**1.14**	**9.2**	**51**	**8.7**
=	**=**	2001	**0.540**	**48.5**	**7**	**1.15**	**9.9**	**53**	**8.1**
$D(r)$ from file	1.47e20	1001	0.310	50.1	23	1.12	5.7		11.7
=	=	=	**0.546**	**49.1**	**19**	**1.17**	**8.3**	**47**	**9.4**
=	=	2001	0.287	49.9	10	1.13	6.0		11.5
=	2.00e20	1001	0.317	53.2	39	1.06	3.4		12.3
=	**=**	**=**	**0.532**	**52.6**	**35**	**1.11**	**5.7**	**38**	**10.4**
+ n_Z^{min}= - 1e16	=	=	0.340	53.3	38	1.07	3.5		12.1
$D(r)$ from formula	1.47e20	1001	0.383	47.9	30	1.19	11.6		6.4
= (*)	=	=	**0.727**	**42.8**	**29**	**1.26**	**19**	**87**	**0.5**
=	=	2001	0.347	47.4	18	1.20	12.5		5.7

t_{END} is the time when the simulation ends [2000, (*) 9000 or **10000** steps limit reached]

E_{cons} is the absolute value of the relative conservation error for impurities in the main plasma

P_{rad}^{MAIN} includes impurities only (no bremsstrahlung, no cyclotron loss)

X_{rad}^{MAIN} is the fraction of input power radiated in MAIN and includes all losses (impurities, bremsstrahlung, cyclotron)

4.1 Results of the reference run

The evolution of several relevant quantities is shown in Fig.5. Notice that the time step has to be suddenly reduced at a certain time. Negative impurity densities begin to appear, and a minimum acceptable value of $n_Z^{min} = -1e15\ m^{-3}$ was set for most of the runs presented here. This problem causes indeed the major, until now unavoidable, burden of the computation, requiring a huge number of time steps before a steady state is reached. However, it is clearly seen from the time evolution that the first part of the simulation, with large time step, is also fairly inaccurate. In a single case (see Table 2) a run was repeated with $n_Z^{min} = -1e16\ m^{-3}$ and gave similar results.

Temperatures at the LCMS and at the FW/limiter increase as the input power increases and then saturate as the losses begin to increase. The incoming neutral impurity flux from SOL to MAIN increases rapidly because of increased sputtering, then the outgoing charged impurity flux starts to increase and tends to compensate the former at steady state. The residual difference between the two is due to spatial discretization errors and is indeed reduced as soon as one increases the number of mesh points in the main plasma (from, say, 1000, which is typically used, to 2000, see Table 2). Notice finally that the fixed amount of power loss due to bremsstrahlung and cyclotron radiation gives the pedestal in X_{rad}^{MAIN}. Most (~2/3) of the SOL losses, however, come from impurities recycling near the FW/limiter (see Appendix D) and as such our prediction may suffer from the uncertainties of that model [3].

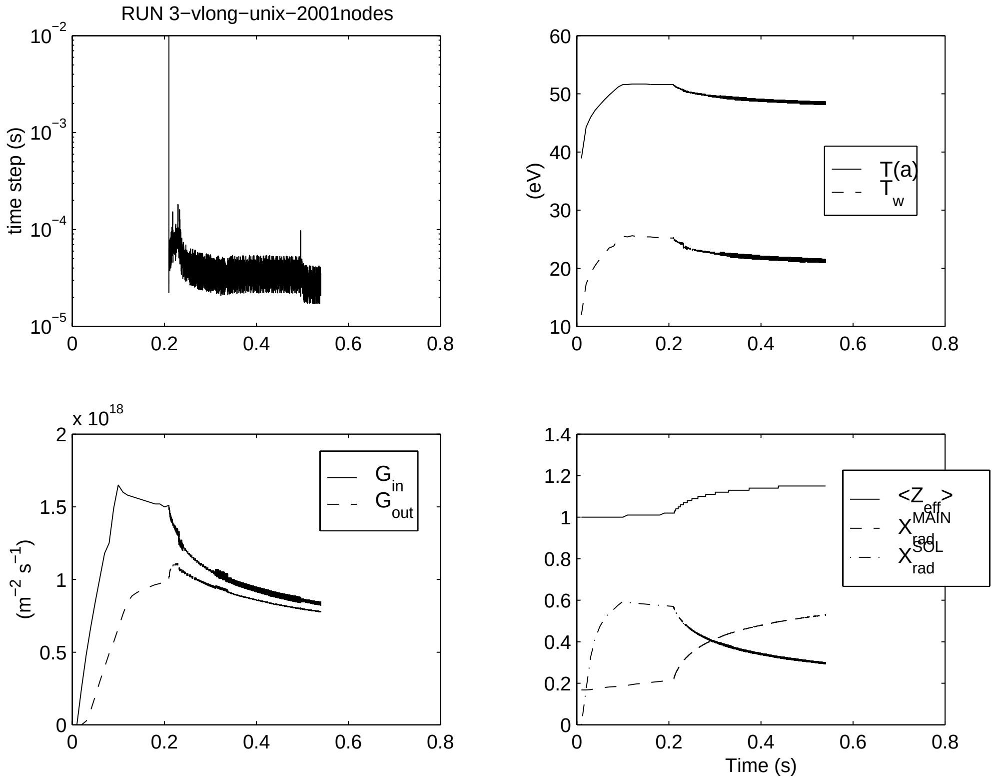

Figure 5 *Evolution in time of several relevant quantities. Reference case.*

The radial profile of each ionization stage from MoI (neutral) to MoXLIII (fully ionized) is shown in Fig.6 and refers to the final time of the simulation (note the differences in the x- and y-axes between different subplots). The lowest ionization stages and in particular the driving ionization source of neutral impurities require an extremely fine mesh near the plasma edge (the density of neutral impurities decreases by about 10 orders of magnitude over the first 3mm of plasma!). This notwithstanding some oscillations and a few negative values appear. For some scenarios spatial convergence was checked (see Table 2) and appears to be ok.

These profiles result in a distribution of Z_{eff} and of impurity radiated power density in the main plasma as shown in Figs.7a,b. The total radiated power fraction is ~ 80%, with ~50% in the main plasma and ~30% in the SOL. The outermost 1/3 of the main plasma is responsible for about 50% of the main plasma impurity-related losses, and the innermost 2/3 of the main plasma account for only about 1/4 of the total radiation loss. The spikes in the power density come also from the use of different formulas for radiation in different plasma regions.

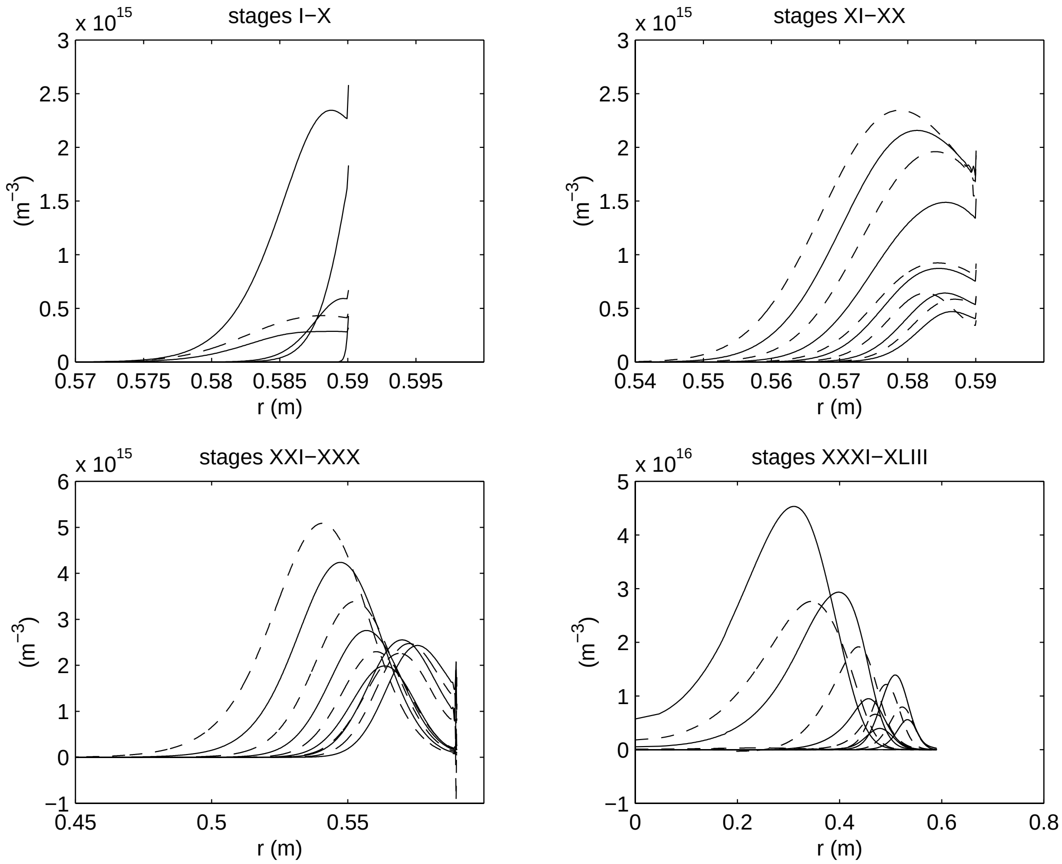

Figure 6 *Radial profiles in main plasma of all ionization stages of Mo at last time step*

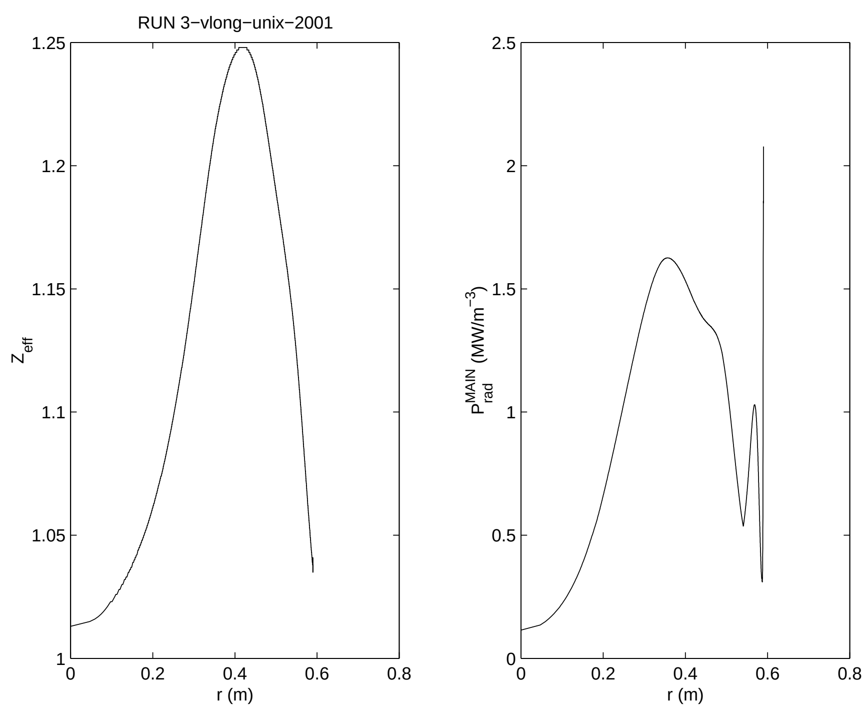

Figure 7a *Radial profiles in main plasma of Z_{eff} and of impurity radiated power density*

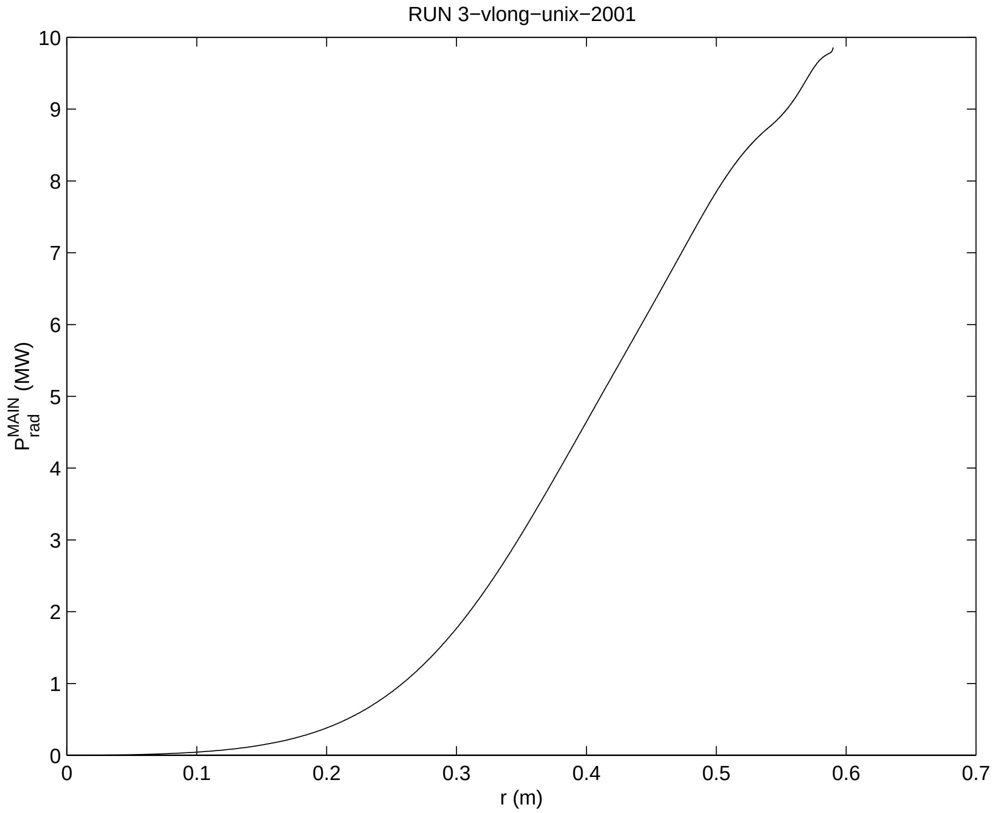

Figure 7b *Radial profile in main plasma of impurity radiated power*

4.2 Effect of different edge density $n_e(a)$ and/or density profile $n_e(r)$

The effect of different density profiles with the same edge density (1.47e20), as shown in Fig.2 was investigated. Differences in the results (see Table 2) turn out to be small (typically ≤ 10%).

A more sensitive parameter appears to be the edge electron density, which determines the screening capability of the SOL. We used here two parameterized profiles with the same peak and average but different $n_e(a)$, 1.47e20 and 2.e20 respectively, as shown in Fig.2. The ~36% increase of the edge density effectively leads to increased screening with a reduction of ($\langle Z_{eff} \rangle - 1$) by ~27% and a reduction of the impurity radiated power in MAIN by ~38% (see Table 2).

4.3 Effect of different profiles of the impurity diffusion coefficient D(r)

The effect of a different shape of D(r) (see Fig.4) was investigated using a parameterized density profile with $n_e(a)$=1.47e20. The results of this comparison are also summarized in Table 2, and the differences in $Z_{eff}(r)$ and radiated power density are shown in Fig.8 below. We notice from Fig.8 that the lower D in the 0.4m < r < 0.6m region leads to a stronger confinement of impurities, thereby increasing ($<Z_{eff}>$ – 1) by ~50% and P_{rad}^{MAIN} by about a factor 2. In particular, the innermost 1/3 of the MAIN radiates now through impurities ~1.8MW instead of 0.35MW of the reference case. The total radiated power is however comparable (see Table 2) because P_{rad}^{SOL} simultaneously decreases drastically.

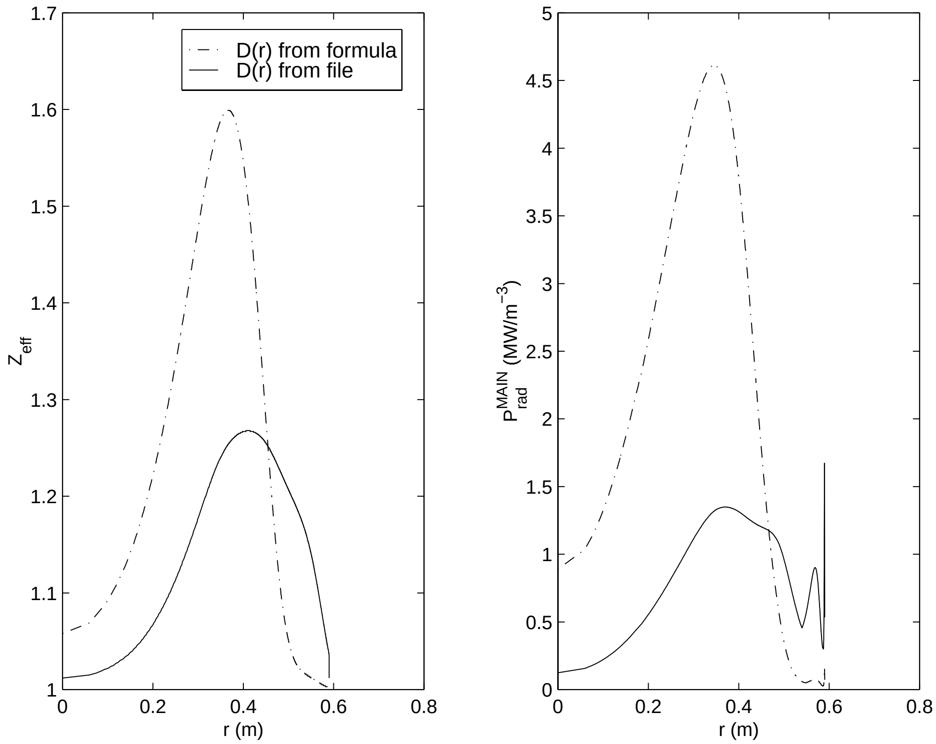

Figure 8 *Comparison between results obtained with different profiles of D(r) as in Fig.4*

5. Conclusion and perspective

Impurity concentration and radiated power in IGNITOR have been computed with a self-consistent model implemented in the SCOUT code. A Mo limiter/FW was assumed. $<Z_{eff}>$ was computed to be in the range 1.10-1.25, while the radiated power fraction in the main was between 40% and 80% depending on different assumptions.

A rather strong sensitivity of the results was shown on the edge plasma density and on the radial profile of the impurity diffusion coefficient in the MAIN plasma. The actual choice of diffusion and inward pinch for these simulations, however, should undergo further scrutiny.

In perspective, validation of SCOUT could be extended to limited Alcator C-Mod discharges, provided the dominating impurity species (Mo?) can be identified.

Compatibility of the present results with computations concentrating on the fuel component, e.g. [9], is only partial: D(r), V_{in}(r) and n_e(r) profiles are taken from [9] but <u>no feedback of the present results on [9] was investigated</u>. This issue should be addressed in the future.

Neoclassical effects are not included at present in the main plasma portion of the model but they could obviously be important, particularly for high-Z impurities.

References

[1] B.Coppi and the IGNITOR Group, Proc.17th SOFT, Vol.2 (1993) 1621.
[2] C.Ferro and R.Zanino, *J. Nucl. Mater*. **196-198** (1992) 321.
[3] R.Zanino and C.Ferro, *Contrib. Plasma Phys.* **34** (1994) 337.
[4] R.Zanino and C.Ferro, *Europhys. Conf. Abstracts* **18B** (1994) 822.
[5] R.Zanino and C.Ferro, *Contrib. Plasma Phys.* **36** (1996) 260.
[6] M.L.Apicella, et al., *Nucl. Fusion* **37** (1997) 381.
[7] R.Zanino, C.Ferro and M.Frassinesi, presented at the 6-th Plasma Edge Theory Conference, September 15-17 1997, Oxford, UK.
[8] R.Zanino, C.Ferro, M.Frassinesi and M.Leigheb, to appear in *J. Nucl. Mater.* (1998).
[9] A.Airoldi and G.Cenacchi, *Nucl. Fusion* **37** (1997) 1117.

Appendix A - Equilibrium data [from Airoldi and Cenacchi]

R	Z	PPDS	ANGFI	RP	ZP
1.8100E+00	0.0000E+00	2.1872E-02	–3.1416E+00	1.7881E+00	–9.6299E-04
1.8086E+00	3.8010E-02	2.1454E-02	–3.1361E+00	1.7871E+00	3.7721E-02
1.8054E+00	7.6361E-02	2.1331E-02	3.1378E+00	1.7842E+00	7.3328E-02
1.8004E+00	1.1451E-01	2.1465E-02	3.1302E+00	1.7791E+00	1.1168E-01
1.7937E+00	1.5239E-01	2.1855E-02	3.1237E+00	1.7726E+00	1.4680E-01
1.7853E+00	1.8991E-01	2.2415E-02	3.1187E+00	1.7636E+00	1.8444E-01
1.7753E+00	2.2702E-01	2.3185E-02	3.1158E+00	1.7536E+00	2.1875E-01
1.7636E+00	2.6364E-01	2.3983E-02	3.1148E+00	1.7411E+00	2.5538E-01
1.7505E+00	2.9970E-01	2.4902E-02	3.1160E+00	1.7270E+00	2.9142E-01
1.7360E+00	3.3513E-01	2.5748E-02	3.1190E+00	1.7127E+00	3.2413E-01
1.7200E+00	3.6989E-01	2.6610E-02	3.1239E+00	1.6958E+00	3.5895E-01
1.7028E+00	4.0389E-01	2.7318E-02	3.1303E+00	1.6790E+00	3.9050E-01
1.6845E+00	4.3708E-01	2.7966E-02	3.1381E+00	1.6612E+00	4.2149E-01
1.6650E+00	4.6940E-01	2.8377E-02	–3.1362E+00	1.6409E+00	4.5442E-01
1.6446E+00	5.0080E-01	2.8645E-02	–3.1264E+00	1.6212E+00	4.8422E-01
1.6232E+00	5.3122E-01	2.8730E-02	–3.1163E+00	1.6007E+00	5.1345E-01
1.6011E+00	5.6060E-01	2.8603E-02	–3.1060E+00	1.5793E+00	5.4210E-01
1.5784E+00	5.8890E-01	2.8253E-02	–3.0957E+00	1.5572E+00	5.7015E-01
1.5550E+00	6.1606E-01	2.7691E-02	–3.0859E+00	1.5343E+00	5.9761E-01
1.5312E+00	6.4203E-01	2.6967E-02	–3.0767E+00	1.5107E+00	6.2442E-01
1.5070E+00	6.6677E-01	2.6073E-02	–3.0683E+00	1.4885E+00	6.4842E-01
1.4825E+00	6.9024E-01	2.5052E-02	–3.0607E+00	1.4655E+00	6.7181E-01
1.4579E+00	7.1239E-01	2.3880E-02	–3.0539E+00	1.4420E+00	6.9456E-01
1.4331E+00	7.3318E-01	2.2603E-02	–3.0481E+00	1.4178E+00	7.1660E-01
1.4084E+00	7.5258E-01	2.1236E-02	–3.0432E+00	1.3952E+00	7.3598E-01
1.3838E+00	7.7054E-01	1.9796E-02	–3.0392E+00	1.3720E+00	7.5465E-01
1.3593E+00	7.8704E-01	1.8299E-02	–3.0361E+00	1.3482E+00	7.7252E-01
1.3351E+00	8.0205E-01	1.6758E-02	–3.0343E+00	1.3262E+00	7.8784E-01
1.3111E+00	8.1554E-01	1.5191E-02	–3.0332E+00	1.3036E+00	8.0233E-01
1.2876E+00	8.2747E-01	1.3611E-02	–3.0338E+00	1.2805E+00	8.1585E-01
1.2645E+00	8.3784E-01	1.2035E-02	–3.0356E+00	1.2594E+00	8.2691E-01
1.2418E+00	8.4661E-01	1.0482E-02	–3.0394E+00	1.2378E+00	8.3692E-01
1.2197E+00	8.5377E-01	9.0630E-03	–3.0466E+00	1.2157E+00	8.4565E-01
1.1981E+00	8.5930E-01	7.6456E-03	–3.0570E+00	1.1958E+00	8.5201E-01
1.1772E+00	8.6319E-01	6.4593E-03	–3.0713E+00	1.1756E+00	8.5693E-01
1.1568E+00	8.6542E-01	5.6318E-03	–3.0899E+00	1.1550E+00	8.6011E-01
1.1372E+00	8.6599E-01	4.8185E-03	–3.1130E+00	1.1372E+00	8.6118E-01

1.1182E+00	8.6490E-01	4.5697E-03	–3.1399E+00	1.1193E+00	8.6047E-01
1.1000E+00	8.6214E-01	4.6985E-03	3.1145E+00	1.1017E+00	8.5777E-01
1.0824E+00	8.5772E-01	5.1979E-03	3.0866E+00	1.0845E+00	8.5294E-01
1.0657E+00	8.5165E-01	6.1128E-03	3.0623E+00	1.0680E+00	8.4601E-01
1.0497E+00	8.4395E-01	7.3755E-03	3.0442E+00	1.0525E+00	8.3715E-01
1.0345E+00	8.3465E-01	8.5691E-03	3.0338E+00	1.0404E+00	8.2849E-01
1.0200E+00	8.2376E-01	9.8074E-03	3.0309E+00	1.0269E+00	8.1680E-01
1.0063E+00	8.1134E-01	1.0990E-02	3.0340E+00	1.0145E+00	8.0398E-01
9.9340E-01	7.9739E-01	1.2014E-02	3.0418E+00	1.0031E+00	7.9026E-01
9.8119E-01	7.8197E-01	1.2902E-02	3.0525E+00	9.9254E-01	7.7584E-01
9.6968E-01	7.6509E-01	1.3424E-02	3.0649E+00	9.8127E-01	7.5831E-01
9.5886E-01	7.4680E-01	1.3783E-02	3.0777E+00	9.7096E-01	7.4020E-01
9.4869E-01	7.2711E-01	1.3933E-02	3.0906E+00	9.6150E-01	7.2163E-01
9.3916E-01	7.0607E-01	1.3848E-02	3.1026E+00	9.5160E-01	6.9998E-01
9.3024E-01	6.8372E-01	1.3577E-02	3.1141E+00	9.4253E-01	6.7795E-01
9.2190E-01	6.6009E-01	1.3082E-02	3.1245E+00	9.3421E-01	6.5564E-01
9.1414E-01	6.3522E-01	1.2512E-02	3.1338E+00	9.2562E-01	6.3026E-01
9.0691E-01	6.0916E-01	1.1756E-02	–3.1410E+00	9.1776E-01	6.0464E-01
9.0021E-01	5.8196E-01	1.0812E-02	–3.1345E+00	9.1056E-01	5.7883E-01
8.9401E-01	5.5366E-01	9.9502E-03	–3.1290E+00	9.0325E-01	5.4997E-01
8.8829E-01	5.2431E-01	8.9591E-03	–3.1248E+00	8.9724E-01	5.2386E-01
8.8303E-01	4.9398E-01	7.8267E-03	–3.1223E+00	8.9055E-01	4.9181E-01
8.7823E-01	4.6272E-01	6.8490E-03	–3.1209E+00	8.8507E-01	4.6254E-01
8.7384E-01	4.3058E-01	5.8097E-03	–3.1201E+00	8.7964E-01	4.3025E-01
8.6988E-01	3.9762E-01	4.9259E-03	–3.1204E+00	8.7480E-01	3.9786E-01
8.6630E-01	3.6392E-01	4.0992E-03	–3.1218E+00	8.7013E-01	3.6244E-01
8.6312E-01	3.2952E-01	3.2894E-03	–3.1238E+00	8.6638E-01	3.2991E-01
8.6030E-01	2.9450E-01	2.5349E-03	–3.1259E+00	8.6283E-01	2.9436E-01
8.5784E-01	2.5892E-01	1.9513E-03	–3.1277E+00	8.5979E-01	2.5876E-01
8.5574E-01	2.2285E-01	1.4934E-03	–3.1290E+00	8.5720E-01	2.2313E-01
8.5397E-01	1.8636E-01	1.5450E-03	–3.1302E+00	8.5504E-01	1.8747E-01
8.5253E-01	1.4951E-01	9.3722E-04	–3.1325E+00	8.5315E-01	1.4881E-01
8.5142E-01	1.1238E-01	8.2769E-04	–3.1357E+00	8.5181E-01	1.1311E-01
8.5063E-01	7.5041E-02	6.3581E-04	–3.1371E+00	8.5078E-01	7.4424E-02
8.5016E-01	3.7556E-02	1.1476E-03	–3.1385E+00	8.5021E-01	3.8702E-02
8.5000E-01	0.0000E+00	2.9772E-03	3.1416E+00	8.5000E-01	2.9772E-03

Appendix B - Output units for SCOUT code

Unit #	File name (.dat)	File content (columns)
92	**Finale**	***Summary of informations on completed run***
95	**Param**	$t, n_e(a), n_{ew}, T(a), T_w$
96	**Powers**	$t, \Gamma_{0z}^{sol \rightarrow main}, \Gamma_z^{main \rightarrow sol}, P^{main \rightarrow sol}/P_{in}, P_{rad}^{sol}/P_{in}$
97	**Zeffdet**	$t, \Delta t, <Z_{eff}>$, **step #**
93	**Sout1 (*)**	$r, n_e, n_i, n_{Z,} T$, **node #**
94	**Sout2 (*)**	$r, Z_{eff}, P_{rad}^{main}$ [W/m^3], P_{rad}^{main} [W]
43	**Therload**	$Q_{tot}, Q_{conv}, <Q>, Q_{max}$
45	**D_and_vin**	r, D, V_{in} ***(from input)***
472	**Profilia**	$r, n_Z^{I}, \ldots, n_Z^{V}$
473	**Profilib**	$r, n_Z^{VI}, \ldots, n_Z^{X}$
474	**Profilic**	$r, n_Z^{XI}, \ldots, n_Z^{XV}$
475	**Profilid**	$r, n_Z^{XVI}, \ldots, n_Z^{XX}$
476	**Profilie**	$r, n_Z^{XXI}, \ldots, n_Z^{XXV}$
477	**Profilif**	$r, n_Z^{XXVI}, \ldots, n_Z^{XXX}$
478	**Profilig**	$r, n_Z^{XXI}, \ldots, n_Z^{XXXV}$
479	**Profilih**	$r, n_Z^{XXXVI}, \ldots, n_Z^{XL}$
480	**Profilii**	$r, n_Z^{XLI}, \ldots, n_Z^{XLIII}$

All radial profiles are given @ $t=t_{END}$ except in (*), where they are updated every 10 time steps

Appendix C - Input files for reference run with SCOUT

```
*               ADT FILE
*tramp;rnthres;sstol;iupdown;neuquasi;iacc;icoll;limiter
*
*
1.d-1
*
-1.d9
*
2.d-3
*
0
*
4
*if iacc=1 r=1;if iacc=0 nessuna termalizzazione
1
*if icoll=1 ioni collisionali (m=0.75)
1
*if limiter=0 poloidale; =1 ftu-toroidale; =2 ignitor
2
```

```
* Data for scout_main.for:SCMA ignitor
* istandalone; LT; R, RMAG; DK, dbedge; VD; rn00; METRIC; NTE, DET.
*
*
0
*Numero atomico impurezza (Ni=28, Mo=42)
42
1.d-24          radsol Mo;    6.d-25        radsol Ni
*Raggio minore (calcolato come Vol/Sup) e maggiore in CGS
59.0d0
132.5d0
*ATTENZIONE: porre dbedge=0.d0 per Bohm's scaling (ORIG. .4 e .8)
1.d4
1.d4
*radius1 e radius2(frazione raggio minore)
0.33d0
0.5d0
*inward pinch multiplier
-1.d2
* RN00 IN #/CM3 valore usato per standalone 9.4748d7;1.11d10 per Carloedged
0.d0
*
3
*
10000
1.d-2
1.d-6     detmin
50        ncheck
1.d-2     detmax
1.1d0     dtmul
1.5d0     dtred
```

```
*Data for scout_sol.for:SCSO
*
```

*   SHOT ignitor
efflim
0.639d0
corrlc
1.5d0
bt
13.0d0
q(a)
3.6d0
gadis
2.d0
amach
0.3d0
amu
2.5d0
gamma
9.5d0
cd, avld????, avd, ct, avt
11.0d20
4.65d19
5.0d20
11.0d3
5.5d3
b, c
0.008d0
0.0235d0
am2, u0 (am2=95.9 u0=6.8 sono per Mo, per Ni am2=58.7 u0=4.3)
95.9d0
6.8d0
cpot (11.26 for C, 7.635 for Ni, 7.099 for Mo <-- http://wulff.mit.edu/pt/)
7.099
zrec,zefsol
1.d0
2.d0
pin
27.3d6
artssy
0.99d0
tol, imax, thetat
1.d-2
1000
2.d-2
dbhm
3.d0
psdcnv
0.65d0
v0i
3.d4

Appendix D - Output file finale.dat for reference run with SCOUT (2001 nodes)

LAMBDA_N 0.239D-01(m)   NE(A) 0.147D+15   n_e(wall) 0.169D+21
TE(A) 0.482D+02(eV)   T_e(wall) 0.210D+02(eV)
ZEFF 0.115D+01   Prad (%) 0.829D+02   PradSOL (%) 0.300D+02
PBREM 0.410D+07   PRAD_MAIN   0.98564890D+07
PRAD_SOL(1) 0.264D+07   PRAD_SOL(2) 0.554D+07
SIMYI 0.160D-02   SIMYZ 0.116D+01   SIMYZR 0.724D-03
RATIO OF EDGE DENSITIES 0.150D-03   ETA 0.180D-01
F_rec/F_i 0.230D-03   Mach_rec 0.233D-01   dz_rec/dz(a) 0.226D+09
lambda_r 0.956D-02   lambda_z 0.194D-03